Received 31 August 2020; revised 30 September 2020; accepted 21 October 2020. Date of publication 27 October 2020; date of current version 17 November 2020.

Digital Object Identifier 10.1109/OJAP.2020.3034051

Low-Cost S-Band Reconfigurable Monopole/Patch Antenna for CubeSats

ALEXANDER D. JOHNSON (Member, IEEE), VIGNESH MANOHAR (Student Member, IEEE), SATHEESH BOJJA VENKATAKRISHNAN (Member, IEEE), AND JOHN L. VOLAKIS (Fellow, IEEE)

Department of Electrical and Computer Engineering, Florida International University, Miami, FL 33174, USA

CORRESPONDING AUTHOR: V. MANOHAR (e-mail: vmanohar@fiu.edu)

This work was supported by the Air Force Office of Scientific Research under Grant FA9550-19-1-0290.

ABSTRACT The development of reconfigurable antennas compatible with a CubeSat form factor can aid several space missions. Often, satellite missions require multiple wireless links with the same radio, but the design of such antennas is challenging due to the mechanical constraints and the limited power aboard a CubeSat. In this article, we present a unique reconfigurable antenna concept enabled by adhesive polyimide tapes. The presented antenna can switch from a conventional patch to a monopole-like antenna with minimal actuation complexity. This reconfiguration provides choices for polarization, pattern, and gain without use of active components for size, cost and power consumption reductions. The frequency of operation is S-band (2.4 GHz), and the antenna achieves $S_{11} < -10$ dB for both reconfiguration states. Measurements compare well with simulations in both states.

INDEX TERMS Antennas, omnidirectional antennas, directive antennas, patch antennas, satellite antennas, antenna radiation patterns.

I. INTRODUCTION

CUBESATS represent a class of low weight (<1.33 kg) satellites that can be as small as $10 \times 10 \times 10$ cm^3 in volume (commonly represented as 1U). Their small size and weight significantly reduces launch costs, thereby enabling the vision of a satellite constellation in space [1]. Indeed, several recent CubeSat constellation missions have been proposed including the RainCube precipitation radar [2], [3], Internet of Space [4], [5], deep space missions [6]–[8], and so on.

For multi-functional radars and communications antennas, achieving reconfiguration within the CubeSat form factor is challenging due to space limitations. Existing methods for physically reconfiguring antennas include origami folding [9], hinges [8], [10], spring forces [11], [12], soft robotics [13], and telescopic actuation [14]. However, these techniques may add significant mechanical complexity, making it difficult to scale. With this in mind, herewith we investigate another antenna design technique. As opposed to strict Origami methods, the presented method uses adhesive polyimide tapes *and* folding to achieve its design goals, for an added layer of tunability in antenna design. For example, 3 dimensional origami methods are often limited since any addition in the normal direction of the sheet's plane inhibits their reconfiguration. This limitation is not present in our design, which enables the presented antenna : a polarization reconfigurable patch/monopole hybrid that shares the same microstrip ground plane and feed. Such a concept was presented recently [15], however, it relied on a remote light source for reconfiguration. The presented antenna reconfiguration employs a new approach and uses space qualified materials [16] with robust actuation. As S-band frequencies are popular for CubeSat communications [17], we select 2.4 GHz as the operation frequency. The antenna can reconfigure its pattern from that of a conventional patch to a dipole (see Fig. 1). This seemingly intuitive reconfiguration can enable the CubeSat to form a nearly isotropic link since the monopole antenna has maximum radiation along the direction where the patch's radiation is weak. One notable application of this design relates to its use in CubeSat constellations, where it is essential for adjacent satellites to form a communication link in addition to providing illumination towards Earth's surface. Several review articles provide an excellent description of various patch and dipole antennas

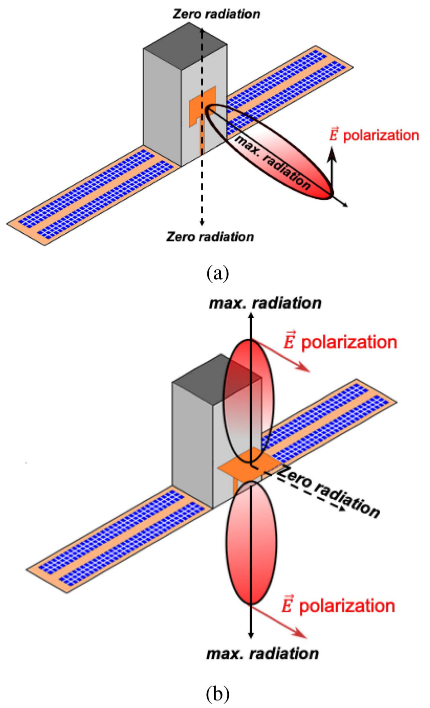

FIGURE 1. Illustration of the S-band reconfigurable antenna enabled by polyimide tapes on a 6U CubeSat in (a) 'patch mode' operation and (b) 'monopole mode' operation. This concept can seamlessly switch between radiation patterns and polarizations, enabling the same radio to meet the RF specifications for different applications.

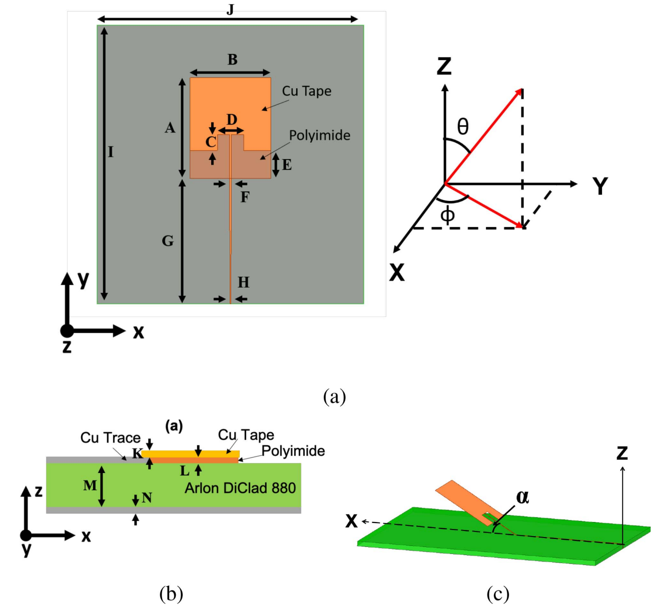

FIGURE 2. Dimensions of the reconfigurable patch/monopole design (a) top view, (b) profile view and (c) the reconfiguration mechanism by altering α.

developed for CubeSats [18]–[22]. A detailed survey of patch antennas for CubeSats and nanosats is provided in [23]. However, merging the capabilities of patch and dipole antennas to facilitate CubeSat missions has not been reported to the best our knowledge.

II. HYBRID PATCH/MONOPOLE ANTENNA DESIGN

A. DESIGN CONCEPTUALIZATION

The most challenging aspect of reconfigurable antenna design is the mechanical realization of the reconfiguration mechanism. For our proposed design, we use a 3.175 mm (125 mil) thick Rogers Arlon DiClad 880 substrate having $\epsilon_r = 2.2$. To form the feed, a microstrip line is etched on the top of this substrate as the first section of the feed-line. The patch geometry and second section of the feed-line is formed using copper tape, and a strip of 0.127 mm (5 mil) thick Polyimide tape as depicted in Fig. 2. This polyimide/patch layer attaches to the etched feed line section on the board through adhesives inherent to the Polyimide tape. A second layer of tape is placed on the bottom face of the patch to cover the excess adhesives. The geometry of the antenna along with the stackup is shown in Fig. 2. Notably, The polyimide layer provides the required mechanical rigidity to our antenna. The next section describes the parameter choices to achieve the desired performance.

B. INITIAL DESIGN EQUATIONS

The patch antenna width and length were initially set using standard formulae [24], [25].

$$W = \frac{c}{2f_r}\sqrt{\frac{2}{\epsilon_r + 1}} \tag{1}$$

$$\epsilon_{eff} = \frac{\epsilon_r + 1}{2} + \frac{\epsilon_r - 1}{2}[1 + 12h/W]^{-0.5} \tag{2}$$

$$\Delta L = 0.412\frac{(\epsilon_{eff} + 0.3)(W/h + 0.264)}{(\epsilon_{eff} - 0.258)(W/h + 0.8)} \tag{3}$$

$$L = \frac{c}{2f_r\sqrt{\epsilon_{eff}}} - 2\Delta L \tag{4}$$

In the above, ϵ_{eff} is the effective dielectric constant of the medium, ΔL is the added effective electric length due to the fringing fields, and $f_r = 2.4$ GHz. Starting with the above equations, feed line and notch dimensions were optimized to achieve 50Ω input impedance matching at the resonant frequency. The same patch was then 'lifted' off the substrate using the hinge created by the adhesive at the feed line junction to achieve the monopole state of operation.

C. TRADE SPACE

The effect of key parameters on performance were studied in relation to patch and monopole reconfiguration states. The challenge is to find key parameters to easily tune the impedance of the patch and monopole. One such parameter is the size of the feed line notch used to match the microstrip patch impedance. The influence of the notch on impedance is depicted in Fig. 3, and shows that the patch is highly dependent on the notch width and length. On the other hand, the monopole radiator has little dependency on the notch's width. That is, even ±50% variation in the notch width has little

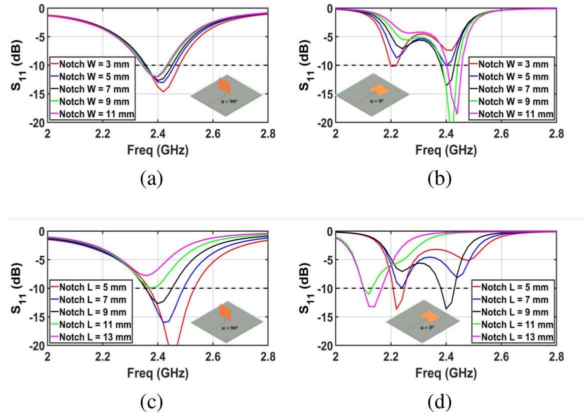

FIGURE 3. Effect of the feed notch width W and length L on impedance matching of the antenna patch and monopole states. (a) Notch width variation at the monopole state and (b) notch width variation at the patch state. (c) Notch length variation at the monopole state, and (d) notch length variation at the patch state.

influence on the matched band of the monopole. However, Fig. 3(c) shows that the monopole impedance has stronger dependency on the notch's length. The same ±50% variation on in notch length significantly affects the impedance behavior.

D. ACTUATION

For the prototype built in this work, the actuation between states was achieved by knotting a thin fishing line at the top edge of the monopole radiator, and pulling on either end to change the antenna's state. In the future, the fish line actuation will be replaced with a high fidelity servo motor for integration with full-framed 6U CubeSats. Along with the force provided by the actuators, the adhesive polyimide tapes allow the antenna to rise up and fall down in a controlled manner. Notably, the inclusion of the two thin layers of polyimide tape gives added structural stability to the copper tape patch/monopole radiator. We also remark that no memory effects are present in the polyimide tapes.

E. FOLD ANGLE TOLERANCE

Actuation misalignment effects on the antenna are shown in Fig. 4. Specifically, the tolerance of the folding angle α was investigated to show the need for accuracy in actuation. It is evident that the patch configuration is highly sensitive to any air gap between the patch radiator and the substrate. This is expected since the impedance of a patch strongly depends on the cavity modes formed between the ground plane and the patch. For α as little as $1°$, the impedance match is significantly impacted. This observation can be used to quickly stop unwanted signals (i.e., high power bursts) from being received. On the other hand, the monopole is resilient to changes in folding angle even upto $\pm 10°$ variation. Fig. 4 shows that the impedance match is hardly affected.

F. SIMULATION RESULTS

The design parameters and the employed coordinate system are shown in Fig. 2 and Table 1. The corresponding 3D

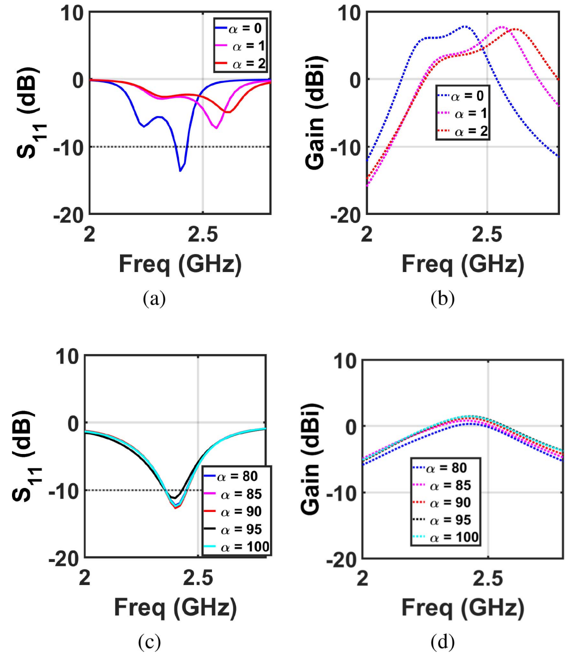

FIGURE 4. Simulated return loss and gain for the antenna in patch and monopole configuration under different folding angles (α). (a) S_{11} and (b) realized gain for values of α close to 0 (patch state). (c) S_{11} and (d) realized gain for α close to 90° (monopole state). The gain is computed at $\theta = 0°$ for the patch and $\theta = 90°$ for the monopole.

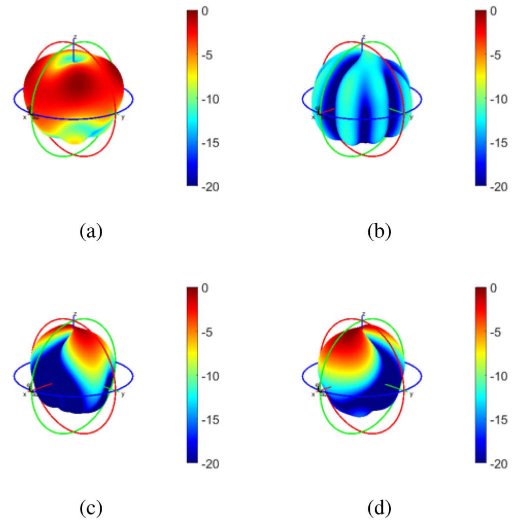

FIGURE 5. 3D normalized radiation patterns (in dB) of the antenna in its monopole and patch states. (a) and (b) illustrate the E_θ and E_ϕ field components at the monopole state and (c) and (d) illustrate the E_θ and E_ϕ field components at the patch antenna state.

TABLE 1. Dimensions (Units: mm) of Antenna in Fig. 2.

A	B	C	D	E	F	G
57.50	46.00	9.00	15.00	16.00	1.00	71.50
H	**I**	**J**	**K**	**L**	**M**	**N**
0.50	159.00	152.00	0.070	0.127	3.175	0.035

far-field patterns are shown in Fig. 5. Also Fig. 6 shows the $\phi = 0°$ patterns (H-plane for the patch antenna). These patterns clearly demonstrate that both the patch and monopole configurations perform as expected. Specifically, the patch

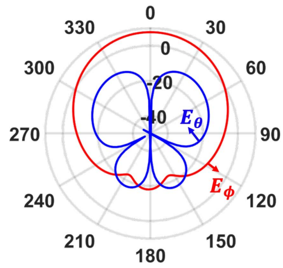

(a)

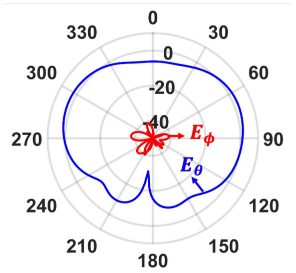

(b)

FIGURE 6. Simulated gain patterns at (a) the patch state and (b) monopole state for the θ and ϕ components.

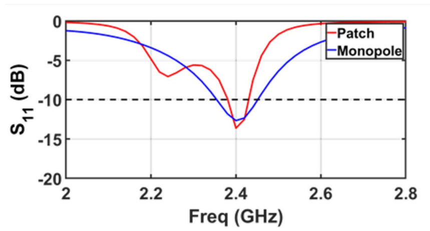

(a)

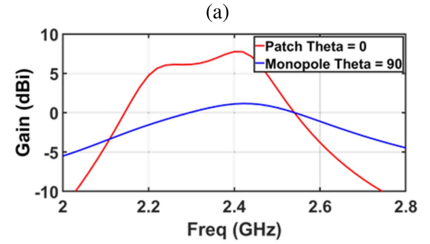

(b)

FIGURE 7. Simulations of the (a) S_{11} and (b) peak realized gain. The peak realized gain refers to $\theta = 0°$ for the patch state and $\theta = 90°$ for the monopole state.

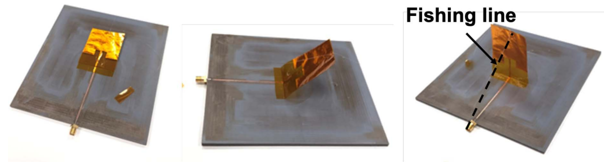

(a) (b) (c)

FIGURE 8. Fabricated antenna while reconfiguring from patch (a) to monopole (c) states. The fishing line served as a proof of concept, and can be replaced by high quality servo motors in the future.

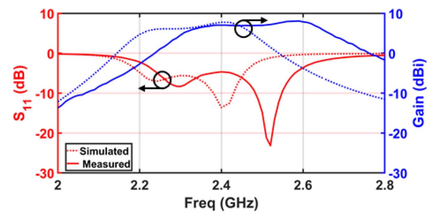

(a)

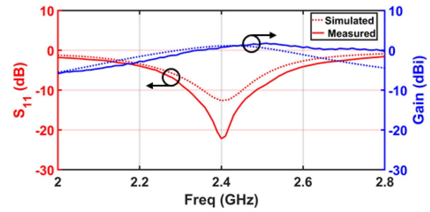

(b)

FIGURE 9. Measured S_{11} and peak realized gain at the (a) patch, and (b) monopole states. The peak realized gain refers to $\theta = 0°$ for the patch and $\theta = 90°$ for the monopole states.

has a maximum along $\theta = 0°$, and has dominant polarization along the y-axis, viz. $\hat{\phi}$ polarized along the $\phi = 0°$ plane, and $\hat{\theta}$ polarized along $\phi = 90°$ plane. The H-plane of the patch exhibited a typical cross-polarization (X-pol) levels of -20 dB as expected [26].

Further, as expected, the monopole antenna has a dominant polarization along $\hat{\theta}$ with a significantly smaller $\hat{\phi}$ component. The monopole has maximum radiation near $\theta = 90°$, and a null depth of approximately -10 dB at $\theta = 0°$. Notably, the finite ground plane is only about 1λ to facilitate integration with a 6U CubeSat. Thus, some deviations from an ideal monopole pattern are expected.

Fig. 7(a) shows that both the patch and monopole configuration of the antenna are resonant at 2.4 GHz as designed. We note that the antenna bandwidth ($S_{11} < -10$ dB) is 2.0% for the patch state, and 4.1% at the monopole state. Fig. 7(b) provides the peak realized gain of the antenna for each state. The peak gain refers to $\theta = 0°$ for the patch and $\theta = 90°$ for the monopole. Notably, the patch shows a gain of 7.7 dBi at $\theta = 0°$ and the monopole has typical gain of 1.2 dBi at $\theta = 90°$.

III. PROTOTYPE FABRICATION AND MEASUREMENTS

The prototype in Fig. 8 was fabricated and measured. The fabricated model had a tolerance of 0.50 mm (20 mil), which is well in accordance with standard low-cost printed circuit board (PCB) processes. The stackup in Fig. 2(b) shows that the folding vertex of the feed line meets the 0.127 mm (5 mil) thick Polyimide tape to act as the folding mechanism. The patch/monopole is constructed from 70 μm (2.75 mil) copper tape, and attached to the polyimide tape (Fig. 2(a)).

The fabricated antenna in Fig. 8 was measured and characterized. Fig. 9(a) shows that at the patch state, the antenna had a slight frequency shift due to fabrication tolerance. Nonetheless, it performs well at 2.4 GHz (the frequency of interest). Notably, the measured bandwidth of 2.6% was slightly greater than 2% due to ohmic losses in the copper features and soldering at the junctions.

Fig. 9(b) shows that the monopole antenna measurements matched quite well with simulations. Here, the measured S_{11} resonates at 2.40 GHz. Also, we observe that the measured bandwidth is 6.9% vs. the 4.1% in simulations. As noted, the bandwidth increase is mainly due to ohmic losses.

The measured gain patterns for the patch and monopole are given in Fig. 10 and compared to simulations. The measured patterns for the patch state agree with simulations, showing a directive beam. Even though the peak gain of 8.0 dBi is at 2.6 GHz, the patch antenna still retains 7.0 dBi gain at

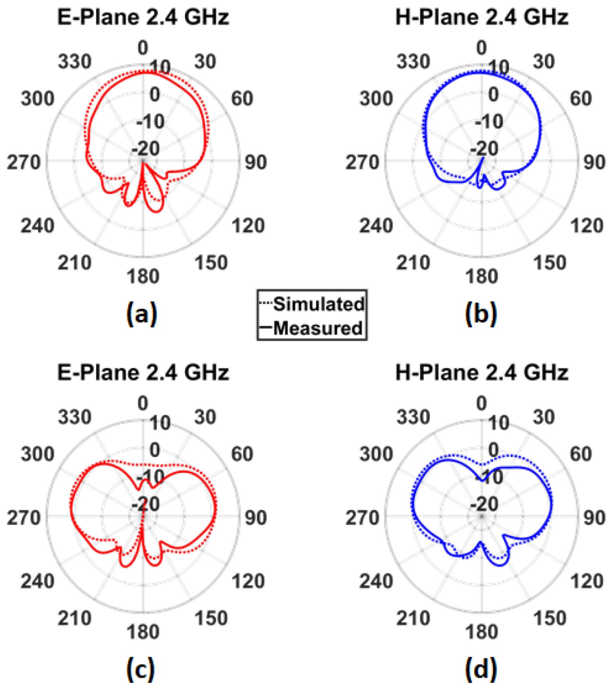

FIGURE 10. (a)&(b) Measured vs. simulated total gain patterns for patch antenna state in E-Plane and H-Plane respectively. (c)&(d) Measured vs. simulated total gain patterns for monopole antenna state in E-Plane and H-Plane respectively.

2.4 GHz. The measured patterns for the monopole also agree with simulations, showing a dipole-like pattern.

IV. CONCLUSION

This article presented a reconfigurable antenna concept in terms of polarization, radiation pattern, and gain level for emerging CubeSats. The presented technique significantly reduces weight, cost and power associated with conventional electronic techniques which use active elements or complex mechanical techniques. The antenna operates in two states: a conventional patch, or a monopole antenna. While these antennas are individually well understood, their operation via a simple reconfiguration is attractive for CubeSat platforms. Studies on key design parameters were included in the paper, and the antenna was fabricated and measured. Measurements are shown to be consistent with simulations Notably, the measurements show antenna operations at 2.4 GHz and achieved 6.9% bandwidth with $S_{11} < -10$ dB in its patch state and 2.6% bandwidth with $S_{11} < -10$ dB in its monopole state. Studies related to antenna space qualification will be developed for specific applications in the future.

REFERENCES

[1] D. Selva and D. Krejci, "A survey and assessment of the capabilities of CubeSat for earth observation," *Acta Astronautica*, vol. 74, pp. 50–68, May/Jun. 2012.

[2] Y. Rahmat-Samii, V. Manohar, J. M. Kovitz, R. E. Hodges, G. Freebury, and E. Peral, "Development of highly constrained 1 m KA-band mesh deployable offset reflector antenna for next generation cubesat radars," *IEEE Trans. Antennas Propag.*, vol. 67, no. 1, pp. 6254–6266, Oct. 2019.

[3] N. Chahat, R. E. Hodges, J. Sauder, M. Thomson, E. Peral, and Y. Rahmat-Samii, "Cubesat deployable Ka-band mesh reflector antenna development for earth science missions," *IEEE Trans. Antennas Propag.*, vol. 64, no. 6, pp. 2083–2093, Jun. 2016.

[4] I. F. Akyildiz and A. Kak, "The Internet of space things/CubeSat: A ubiquitous cyber-physical system for the connected world," *Comput. Netw.*, vol. 150, pp. 134–149, Feb. 2019.

[5] J. Wang, V. Manohar, and Y. Rahmat-Samii, "Enabling the Internet of Things with CubeSat: A review of representative beamsteerable antenna concepts," *IEEE Antennas Propag. Mag.*, early access, Aug. 19, 2020, doi: 10.1109/MAP.2020.3003205.

[6] N. Chahat, R. E. Hodges, J. Sauder, M. Thomson, and Y. Rahmat-Samii, "Deep space network telecommunication CubeSat antenna: Using the deployable Ka-band mesh reflector antenna," *IEEE Antennas Propag. Mag.*, vol. 59, no. 2, pp. 31–38, Apr. 2017.

[7] R. E. Hodges, N. Chahat, D. J. Hoppe, and J. D. Vacchione, "A deployable high-gain antenna bound for mars: Developing a new folded-panel reflectarray for the first cubesat mission to mars," *IEEE Antennas Propag. Mag.*, vol. 59, no. 2, pp. 39–49, Apr. 2017.

[8] N. Chahat, J. Sauder, M. Mitchell, N. Beidleman, and G. Freebury, "One-meter deployable mesh reflector for deep-space network telecommunication at X-band and K_a-band," *IEEE Trans. Antennas Propag.*, vol. 68, no. 2, pp. 727–735, Feb. 2020.

[9] X. Liu, C. L. Zekios, and S. V. Georgakopoulos, "Analysis of a packable and tunable origami multi-radii helical antenna," *IEEE Access*, vol. 7, pp. 13003–13014, 2019.

[10] A. K. Singh and S. Park, "A deployable metamaterial reflectarray antenna for microsatellite application," in *Proc. Int. Symp. Antennas Propag. (ISAP)*, Oct. 2019, pp. 1–2.

[11] E. Decrossas, N. Chahat, P. E. Walkemeyer, and B. S. Velasco, "Deployable circularly polarized UHF printed loop antenna for mars cube one (MarCO) CubeSat," in *Proc. IEEE Int. Symp. Antennas Propag. USNC-URSI Radio Sci. Meeting*, Jul. 2019, pp. 1719–1720.

[12] J. Costantine, Y. Tawk, C. G. Christodoulou, J. Banik, and S. Lane, "CubeSat deployable antenna using bistable composite tape-springs," *IEEE Antennas Wireless Propag. Lett.*, vol. 11, pp. 285–288, 2012.

[13] L. H. Blumenschein, L. T. Gan, J. A. Fan, A. M. Okamura, and E. W. Hawkes, "A tip-extending soft robot enables reconfigurable and deployable antennas," *IEEE Robot. Autom. Lett.*, vol. 3, no. 2, pp. 949–956, Apr. 2018.

[14] A. D. Johnson, J. A. Caripidis, S. B. Venkatakrishnan, M. Ali, and J. L. Volakis, "Deployable inverted-hat monopole with 3:1 constant gain bandwidth," *IEEE Antennas Wireless Propag. Lett.*, vol. 19, no. 6, pp. 935–938, Mar. 2020.

[15] G. J. Hayes, Y. Liu, J. Genzer, G. Lazzi, and M. D. Dickey, "Self-folding origami microstrip antennas," *IEEE Trans. Antennas Propag.*, vol. 62, no. 10, pp. 5416–5419, Aug. 2014.

[16] *NASA Parts Selection List*. Accessed: Aug. 24, 2020. [Online]. Available: https://nepp.nasa.gov/npsl/Wire/insulation_guide.htm

[17] *Executive Summaries*. Accessed: Jul. 12, 2020. [Online]. Available: https://www.nasa.gov/smallsat-institute/sst-soa/executive-summaries

[18] Y. Rahmat-Samii, V. Manohar, and J. M. Kovitz, "For satellites, think small, dream big: A review of recent antenna developments for CubeSat," *IEEE Antennas Propag. Mag.*, vol. 59, no. 2, pp. 22–30, Feb. 2017.

[19] N. Chahat *et al.*, "Advanced cubesat antennas for deep space and earth science missions: A review," *IEEE Antennas Propag. Mag.*, vol. 61, no. 5, pp. 37–46, Oct. 2019.

[20] S. Gao *et al.*, "Antennas for modern small satellites," *IEEE Antennas Propag. Mag.*, vol. 51, no. 4, pp. 40–56, Aug. 2009.

[21] S. Gao, Y. Rahmat-Samii, R. E. Hodges, and X. X. Yang, "Advanced antennas for small satellites," *Proc. IEEE*, vol. 106, no. 3, pp. 391–403, Mar. 2018.

[22] R. Baktur, "Antennas for CubeSat," in *Antenna Engineering Handbook*, 5 ed., J. Volakis, Ed. London, U.K.: McGraw-Hill, ch. 41, 2018.

[23] F. E. Tubbal, R. Raad, K.-W. Chin, and B. Butters, "S-band shorted patch antenna for inter pico satellite communications," in *Proc. 8th Int. Conf. Telecommun. Syst. Services Appl.*, Oct. 2014, pp. 1–4.

[24] C. A. Balanis, *Antenna Theory: Analysis and Design*. New York, NY, USA: Wiley-Intersci., 2005.

[25] D. R. Jackson, "Microstrip antennas," in *Antenna Engineering Handbook*, 5 ed., J. Volakis, Ed. London, U.K.: McGraw-Hill, ch. 7, 2018.

[26] S. Bhardwaj and Y. Rahmat-Samii, “Revisiting the generation of cross-polarization in rectangular patch antennas: A near-field approach,” *IEEE Antennas Propag. Mag.*, vol. 56, no. 1, pp. 14–38, May 2014.

ALEXANDER JOHNSON (Member, IEEE) received the B.S. degree in electrical engineering from Western New England University, Springfield, MA, USA, in 2016, and the M.S. degree in electrical engineering from the Ohio State University, Columbus, OH, USA, in 2017, and the Ph.D. degree in electrical and computer engineering from Florida International University (FIU), Miami, FL, USA, in 2019.

From August 2019 to September 2020, he worked as a Research Assistant Professor with FIU. He is currently a Principal Scientist with BAE Systems, Merrimack, NH, USA. His research interests include novel materials, textile electronics, wideband array apertures, mm-wave phased arrays, and simultaneous transmit and receive (STaR) systems. He was a NASA Research Announcement Fellowship Award recipient, in 2018. He also received an Honorable Mention in the Student Paper Competition at the 2019 IEEE Antenna and Propagation Symposium, and the Student Fellowship Travel Grant Award at the U.S. National Committee for the International Union of Radio Science in 2017 and 2018.

VIGNESH MANOHAR (Student Member, IEEE) received the bachelor’s degree in electronics and telecommunication engineering from the University of Mumbai, in 2013, and the M.S. and Ph.D. degrees in electrical and computer Engineering from the University of California, Los Angeles, in 2016 and 2020, respectively.

He is currently a Postdoctoral Associate with the Department of electrical and computer engineering, Florida International University. His research area focuses on the development of wideband antenna arrays, and deployable high gain aperture antennas for small satellite platforms. He was a recipient of the Outstanding Masters Thesis Award in the Physical and Wave Electronics in 2016, and the Henry Samueli Excellence in Teaching Award in 2020. He received an Honorable Mention in the Altair FEKO Student Competition for his work on stepped reflectors and characterizaition of planar near-field antenna measurements in 2017 and 2018, respectively. He was also the recipient of the 2019 IEEE Electromagnetic Theory Symposium Young Scientist Award for his work on umbrella reflector antenna characterization.

SATHEESH BOJJA VENKATAKRISHNAN (Member, IEEE) was born in Tiruchirappalli, India, in 1987. He received the bachelor’s degree in electronics and communication engineering from the National Institute of Technology, Tiruchirappalli, in 2009, and the M.S. and Ph.D. degrees in electrical engineering from the Ohio State University, Columbus, OH, USA, in 2017.

He was a Scientist with DRDO, India, from 2009 to 2013, working on the development and implementation of active electronic steerable antennas. He is currently a Research Assistant Professor with the Electrical and Computer Engineering, Florida International University. His current research includes receiver design for communication circuits, RF systems, and digital signal processing using FPGAs. He is also working on Simultaneous Transmit and Receive System (STAR), to improve the spectral efficiency. He was a recipient of the IEEE Electromagnetic Theory Symposium Young Scientist Award in 2019. He won the 2nd Prize in International Union of Radio Science General Assembly and Scientific Symposium Student Paper Competition held at Montreal, Canada, in August 2017. He also received the Honorable Mention in the Student Paper Competition at the IEEE Antenna and Propagation Symposium in 2015 and 2016, and the Student Fellowship Travel Grant Award at the U.S. National Committee for the International Union of Radio Science in 2016 and 2017. He has been a Phi Kappa Phi Member, since 2015.

JOHN L. VOLAKIS (Fellow, IEEE) was born in Greece, in May 13, 1956, and immigrated to the USA, in 1973. He received the B.E. degree (*summa cum laude*) from Youngstown State University, Youngstown, OH, USA, in 1978, and the M.Sc. and Ph.D degrees from the Ohio State University, Columbus, OH, in 1979 and 1982, respectively.

He started his career with Rockwell International (currently, Boeing), from 1982 to 1984. In 1984, he was appointed as an Assistant Professor with the University of Michigan, Ann Arbor, MI, USA, and became a Full Professor in 1994. He also served as the Director of the Radiation Laboratory, from 1998 to 2000. From January 2003 to August 2017, he was the Roy and Lois Chope Chair Professor of Engineering with the Ohio State University and served as the Director of the ElectroScience Laboratory, from 2003 to 2016. From August 2017, he is the Dean of the College of Engineering and Computing and a Professor with the Electrical and Computer Engineering, Florida International University. His publications include eight books, 430 journal papers, nearly 900 conference papers, 29 book chapters, and 25 patents/disclosures. Over the years, he carried out research in antennas, wireless communications and propagation, computational methods, electromagnetic compatibility and interference, design optimization, RF materials, multiphysics engineering, millimeter waves, terahertz, and medical sensing. He has coauthored books *Approximate Boundary Conditions in Electromagnetics* in 1995; *Finite Element Methods for Electromagnetics* in 1998; *Antenna Engineering Handbook*, 4th ed., in 2007; *Small Antennas* in 2010; and *Integral Equation Methods for Electromagnetics* in 2011. He has graduated/mentored 95 doctoral students/post-docs with 43 of them receiving Best Paper Awards at conferences. He has serviced in Professional Societies as the President of the IEEE Antennas and Propagation Society in 2004, the Chair of USNC/URSI Commission B, from 2015 to 2017, twice the General Chair of the IEEE Antennas and Propagation Symposium, IEEE APS Distinguished Lecturer, an IEEE APS Fellows Committee Chair, an IEEE-wide Fellows Committee Member and an associate editor of several journals. He received the Research Excellence Award from the University of Michigan, College of Engineering in 1993, the Scott Award from the Ohio State University, College of Engineering for Outstanding Academic Achievement in 2011, the IEEE AP Society C.-T. Tai Teaching Excellence Award in 2011, the IEEE Henning Mentoring Award in 2013, the IEEE Antennas and Propagation Distinguished Achievement Award in 2014, the Ohio State University Distinguished Scholar Award in 2016, the Ohio State University ElectroScience George Sinclair Award in 2017, and the URSI Booker Gold Medal in 2020. He was listed by ISI among the top 250 most referenced authors in 2004, and is a Fellow of ACES and URSI.